Superconducting phase transistor in diffusive four-terminal ferromagnetic Josephson junctions

Mohammad Alidoust,[1,*] Granville Sewell,[2,†] and Jacob Linder[1,‡]

[1]*Department of Physics, Norwegian University of Science and Technology, N-7491 Trondheim, Norway*

[2]*Mathematics Department, University of Texas, El Paso, El Paso, Texas 79968, USA*

(Received 20 October 2011; revised manuscript received 16 March 2012; published 19 April 2012)

We study diffusive magnetic Josephson junctions with four superconducting terminals in the weak proximity limit where the leads are arranged in cross form. Employing the linearized Keldysh-Usadel technique, the anomalous Green's function and Josephson current are analytically obtained based on a quasiclassical theory using the Fourier series method. The derived results may be reduced to nonmagnetic junctions by setting the exchange field equal to zero. We find that increments of the magnetic barrier thickness may cause a reversal of the supercurrent direction flowing into some of the leads, whereas the direction of current flow remains invariant at the others. The reversal direction can be switched by tuning the perpendicular superconducting phases. In the nonmagnetic case, we find that the supercurrent flowing between the leads in one direction can be tuned by changing the superconducting phase difference in the perpendicular direction. These findings suggest the possibility of constructing a nanoscale superconducting phase transistor whose core element consists of the proposed four-terminal Josephson junction with rich switching aspects.

DOI: 10.1103/PhysRevB.85.144520 PACS number(s): 74.50.+r, 74.45.+c, 74.78.Na

I. INTRODUCTION

When a weak link is established between two superconductors, a gradient in the superconducting phases can drive a supercurrent through the system. This Josephson effect[1–3] and the associated current-phase relation in weak links has been investigated extensively in previous literature; see, for example, the comprehensive reviews in Refs. 4 and 5 (see also Refs. 6 and 7 for magnetic Josephson junctions).

The proximity effect between superconductors and normal diffusive metals was first studied by McMillan in 1965.[8] It is known that the electronic properties of a normal metal become altered when placed in proximity with a host superconductor. For instance, the electronic spectrum of the normal metal connected to a superconductor exhibits a minigap.[8–13] Very recently, the key properties of the density of states (DOS) of a normal metal sandwiched between superconductors were employed in an experiment for producing a superconducting quantum interference proximity transistor (SQUIPT).[14] Moreover, superconductor–normal metal–superconductor (S/N/S) Josephson junctions have been studied under nonequilibrium conditions where two additional normal leads are connected to the sandwiched normal layer. It has been demonstrated that this type of S/N/S Josephson junction is able to produce a π junction depending on the voltage applied to the normal sandwiched layer.[15,16] Such π junctions may also be observed in three-terminal junctions.[15,17]

The proximity-induced interplay between superconductivity and ferromagnetism in hybrid structures is also known to establish intriguing physical phenomena. The wave function describing the leakage of Cooper pairs inside a ferromagnet oscillates in a damped fashion. One of the most interesting phenomena in the proximity of ferromagnetism and superconductivity is the 0-π transition, which may occur in superconductor-ferromagnet-superconductor (S/F/S) junctions.[6,18–21] The transition usually occurs over a narrow length $\xi_F = \sqrt{D_F/h}$, in which D_F and h represent the diffusion constant and the exchange field of the sandwiched ferromagnetic layer, respectively. At this crossover point, the minimum energy of the junction is switched between the 0 and π superconducting phase difference by changing the energy scales of the system such as Thouless energy, exchange field, and temperature. Also it has been demonstrated that the spin-flip scattering may render the junction energy a minimum from 0 to π (Refs. 6,22–24) and that the supercurrent itself may become spin polarized if the magnetization texture is inhomogeneous.[25]

So far in the literature, the main emphasis has mostly been on one-dimensional systems where two superconductors are coupled, e.g., via a constriction or diffusive metal. On the other hand, the interplay between multiple superconducting terminals[15] in a Josephson junction would require an extension to higher dimensions.[26,27] This in turn complicates the analytical treatment of the system, and one is usually forced to resort to numerical means within the diffusive regime.[28] It would therefore be of interest to clarify how the transport characteristics of a diffusive ferromagnetic Josephson junction are influenced by the presence of multiple superconducting phase differences, and also to provide an analytical framework for studying such phenomena. Multiterminal Josephson point contacts had intensively been investigated (both ac and dc characteristics) using the Ginzburg-Landau theory[29–31] and were followed by studying the four-terminal S/N/S Josephson junctions in the clean limit via the Eilenberger equations.[26,32,33] Interesting phenomena such as phase dragging (the production of a phase difference between two terminals by means of phase variation between other terminals), magnetic flux transfer, and bistable states were found due to nonlocal coupling and additional degrees of freedom in such classes of Josephson junctions.[26,29,32] Such point contacts also have been fabricated and intensively studied in experiments.[30]

Motivated by this, we consider in this paper a diffusive Josephson junction with four superconducting leads which are arranged in a cruciate form and we study the supercurrent flowing in this junction. The superconducting leads are separated by a metal that may or may not be ferromagnetic. We use the quasiclassical Usadel equations in the diffusive regime

and formulate the current-phase relation as a function of all the available parameters in the system such as superconducting phases in the magnetic junction. We recover the results of Refs. 26 and 32 obtained in the clean S/N/S junctions: namely, when the dimensions L (length) and W (width) of the sandwiched metal are comparable to each other, i.e., $L \simeq W$, the standard sinusoidal supercurrent is strongly modified by all the condensate phases. We also use a phenomenological Ginzburg-Landau theory to confirm our analytical expressions obtained via the quasiclassical framework. In particular, we demonstrate that the Josephson current flowing between leads along one axis may be tuned via the superconducting phase gradient in the perpendicular direction.

Moreover, we find that increments of the magnetic barrier thickness may cause a reversal of the supercurrent direction flowing into some of the leads, whereas the direction of current flow remains invariant at the others. These findings are suggestive in terms of designing a nanoscale superconducting phase transistor where current-switching effects in one direction are possible by variation of the macroscopic superconducting phase in the perpendicular direction, as has also been pointed out in Refs. 33 and 27 for ballistic contacts.

The paper is organized as follows. In Sec. II we present our main analytical findings. In Sec. II A the basic equations of the quasiclassical method are presented and in Sec. II B the cruciate Josephson junction is studied analytically via the Green's function method. We formulate the current-phase relation as a function of the four superconducting phases for a magnetic Josephson junction. In Sec. II C we confirm our results and findings via a macroscopic Ginzburg-Landau theory. In Sec. IV we employ a collocation finite element numerical method[34] (which is explained in detail) and investigate the behavior of the supercurrent, which confirms our analytically derived expressions in Sec. II B and their dependencies on the superconducting U(1) phases; also the behavior of the junction is analyzed in more detail. Section IV is devoted to the study of the supercurrent behavior in S/F/S four-terminal junctions as a function of ferromagnetic barrier thickness. Concluding remarks are finally given in Sec. V.

II. THEORY AND ANALYTICAL DISCUSSIONS

We consider four superconducting leads coupled via a ferromagnetic or normal diffusive metal. As in Fig. 1, the nanoscale diffusive metal is assumed to be located in the xy plane, where $x \in [0,L]$ and $y \in [0,W]$. The four superconducting terminals are assumed to have equal magnitudes for the gap Δ and are connected to each edge of the diffusive strip. The suppression of the pair potential is neglected near interfaces due to a low interface transparency, and the superconducting phases are assumed to be different in each of the four terminals: $\theta_{\rm up}$, $\theta_{\rm down}$, $\theta_{\rm left}$, and $\theta_{\rm right}$. One may expect that superconducting correlations inside the system interfere, resulting in a quite complicated coherent system. The S/F/S system is studied in the diffusive limit and the current-phase relationship is obtained at each terminal similar to clean S/N/S four-terminal junctions.[26,32] In our approach, we start with a magnetic four-terminal Josephson junction and derive our analytical results for the magnetic system. We then may achieve the nonmagnetic Josephson junction characteristics by setting the magnetic exchange field h equal to zero.

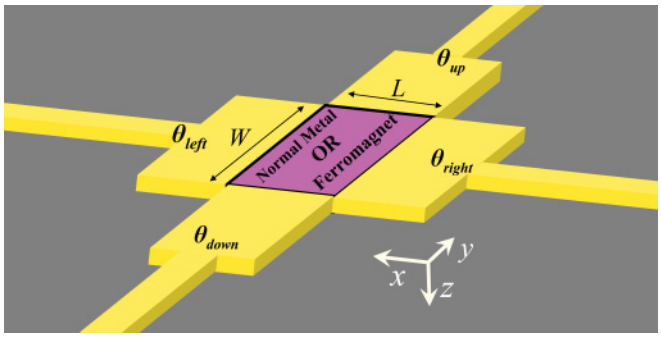

FIG. 1. (Color online) Experimental schematic setup of the cruciate Josephson junction. The junction is assumed to lie in the xy plane with interfaces located at $x = 0, L$ and $y = 0, W$. The four spin-singlet superconductors have different superconducting phases: $\theta_{\rm up}$, $\theta_{\rm down}$, $\theta_{\rm left}$, and $\theta_{\rm right}$. The exchange field $\mathbf{h}$ is assumed to be oriented in the z direction, perpendicular to the sandwiched layer plane.

A. Microscopic Green's function approach

In this section, we present basic equations of the quasiclassical Keldysh-Usadel method. In order to study the transport properties of the proposed four-terminal device, we employ the quasiclassical method. In the diffusive regime, due to the existence of strong scattering sources, quasiparticle momenta are integrated over all directions in space. In this case, the Eilenberger equations reduce to the Usadel equations.[35] Under equilibrium conditions, the system under consideration can be described by a 4×4 matrix propagator in Nambu space: the retarded Green's function G^R. The total Green's function describing the system compactly reads[36]

$$\hat{G}(R,\varepsilon,T) = \begin{pmatrix} G^A & G^K \\ \mathbf{0} & G^R \end{pmatrix}, \quad G^R = \begin{pmatrix} g^R & f^R \\ -\tilde{f} & -\tilde{g} \end{pmatrix}, \quad (1)$$

where the meaning of the $\tilde{\ }$ operation depends on the notation adopted. In our notation, it denotes complex conjugation and a change in sign for the energy argument. The advanced and Keldysh blocks are made from the retarded block by $G^A = -(\tau_3 G^R \tau_3)^\dagger$ and $G^K = \tanh(\beta\varepsilon)(G^R - G^A)$ in which τ_3 is the Pauli matrix and $\beta = k_B T/2$. In the presence of exchange energy $\mathbf{h} = (h_x, h_y, h_z)$ inside the ferromagnetic layer, the Usadel equation can be given by

$$D[\hat{\partial}, \hat{G}[\hat{\partial}, \hat{G}]] + i[\varepsilon\hat{\rho}_3 + \mathrm{diag}[\mathbf{h}\cdot\underline{\sigma}, (\mathbf{h}\cdot\underline{\sigma})^\tau], \hat{G}] = 0, \quad (2)$$

where $\hat{\rho}_3$ and $\underline{\sigma}$ are 4×4 and 2×2 Pauli matrices, respectively. Here D is the diffusive constant of the sandwiched medium. Also, ε is the quasiparticle energy, which is measured from Fermi surface.

The so-called weak proximity regime occurs in the case of very low transparent interfaces or for temperatures near the critical temperature of the superconducting leads. The superconducting correlations leak into the ferromagnetic region weakly and so the normal and anomalous Green's functions can be approximated by $\underline{g} \simeq \underline{1}$ and $\underline{f} \ll \underline{1}$, respectively. In this limit one can linearize the Usadel equation, which yields a

set of uncoupled complex boundary-value partial differential equations. The energy representation is used in this paper; however, one may reach the Matsubara representation by replacing $\varepsilon \to i\omega_n$, where $\omega_n = (2n+1)\pi k_B T$ are Matsubara frequencies. For the sake of simplicity, a uniform exchange field for the ferromagnetic layer is considered throughout the paper; i.e., $\mathbf{h} = (0,0,h_z = h)$. In the weak proximity regime mentioned above, the Green's function reads[24]

$$\hat{G}^R \approx \begin{pmatrix} \underline{1} & \underline{f}^R \\ -\underline{\tilde{f}}^R & -\underline{1} \end{pmatrix}. \tag{3}$$

In fact, we have expanded the Green's function around the bulk solution $\hat{G}_0$ as $\hat{G} \simeq \hat{G}_0 + \hat{f}$, where $\hat{G}_0 = \mathrm{diag}(\underline{1}, -\underline{1})$.[7] The retarded Green's function now can be given by

$$\hat{G}^R = \begin{pmatrix} 1 & 0 & 0 & f_+^R(\varepsilon) \\ 0 & 1 & f_-^R(\varepsilon) & 0 \\ 0 & [-f_+^R(-\varepsilon)]^* & -1 & 0 \\ [-f_-^R(-\varepsilon)]^* & 0 & 0 & -1 \end{pmatrix}. \tag{4}$$

If we assume that the exchange field is uniform throughout the sample and is oriented in the z direction, the Usadel equations reduce to the two-dimensional form as follows:

$$\partial_x^2 f_\pm^R(-\varepsilon) + \partial_y^2 f_\pm^R(-\varepsilon) - \frac{2i(\varepsilon \mp h)}{D} f_\pm^R(-\varepsilon) = 0, \tag{5}$$

$$\partial_x^2 [f_\pm^R(\varepsilon)]^* + \partial_y^2 [f_\pm^R(\varepsilon)]^* - \frac{2i(\varepsilon \pm h)}{D} [f_\pm^R(\varepsilon)]^* = 0. \tag{6}$$

We employ the Kupriyanov-Lukichev boundary conditions at F/S interfaces[37] and control their opacities using a parameter ζ that depends on the resistance of the interface and the diffusive normal region:

$$\zeta(\hat{G}\hat{\partial}\hat{G}) \cdot \hat{\boldsymbol{n}} = [\hat{G}_{\mathrm{BCS}}(\theta), \hat{G}], \tag{7}$$

where $\hat{\boldsymbol{n}}$ is a unit vector denoting the perpendicular direction to an interface. The bulk solution $\hat{G}_{\mathrm{BCS}}$ for an s-wave superconductor is[36]

$$\begin{aligned} \hat{G}^R_{\mathrm{BCS}}(\theta) &= \begin{pmatrix} \mathbf{1}\cosh(\vartheta(\varepsilon)) & i\tau_2 \sinh(\vartheta(\varepsilon)) e^{i\theta} \\ i\tau_2 \sinh(\vartheta(\varepsilon)) e^{-i\theta} & -\mathbf{1}\cosh(\vartheta(\varepsilon)) \end{pmatrix}, \\ \vartheta(\varepsilon) &= \mathrm{arctanh}\left(\frac{|\Delta|}{\varepsilon}\right), \\ s(\varepsilon) &\equiv \sinh(\vartheta(\varepsilon)) e^{i\theta} \\ &= -\Delta\left\{\frac{\mathrm{sgn}(\varepsilon)}{\sqrt{\varepsilon^2 - \Delta^2}}\Theta(\varepsilon^2 - \Delta^2) \right. \\ &\quad \left. - \frac{i}{\sqrt{\Delta^2 - \varepsilon^2}}\Theta(\Delta^2 - \varepsilon^2)\right\} \\ c(\varepsilon) &\equiv \cosh(\vartheta(\varepsilon)) \\ &= \frac{|\varepsilon|}{\sqrt{\varepsilon^2 - \Delta^2}}\Theta(\varepsilon^2 - \Delta^2) \\ &\quad - \frac{i\varepsilon}{\sqrt{\Delta^2 - \varepsilon^2}}\Theta(\Delta^2 - \varepsilon^2). \end{aligned} \tag{8}$$

Here Δ is the superconducting gap in the s-wave superconductors and the Heaviside step function is denoted by $\Theta(\varepsilon)$. In this paper, we have defined $\theta_u, \theta_d, \theta_l, \theta_r$ as the condensate phases in the up, down, left, and right superconductor leads, respectively.

If we now open up the compacted boundary conditions, Eq. (7), at the left F/S interface, for instance, we reach at $x = 0$

$$\begin{aligned} [\zeta\partial_x - c^*(\varepsilon)] f_\pm^R(-\varepsilon) &= \pm s^*(\varepsilon) e^{i\theta_l}, \\ [\zeta\partial_x - c^*(\varepsilon)][f_\pm^R(\varepsilon)]^* &= \mp s^*(\varepsilon) e^{-i\theta_l}, \end{aligned} \tag{9}$$

and at $x = L$

$$\begin{aligned} [\zeta\partial_x + c^*(\varepsilon)] f_\pm^R(-\varepsilon) &= \mp s^*(\varepsilon) e^{i\theta_r}, \\ [\zeta\partial_x + c^*(\varepsilon)][f_\pm^R(\varepsilon)]^* &= \pm s^*(\varepsilon) e^{-i\theta_r}. \end{aligned} \tag{10}$$

Also at $y = 0$

$$\begin{aligned} [\zeta\partial_y - c^*(\varepsilon)] f_\pm^R(-\varepsilon) &= \pm s^*(\varepsilon) e^{i\theta_d}, \\ [\zeta\partial_y - c^*(\varepsilon)][f_\pm^R(\varepsilon)]^* &= \mp s^*(\varepsilon) e^{-i\theta_d}, \end{aligned} \tag{11}$$

and at $y = W$ the boundary condition takes the form

$$\begin{aligned} [\zeta\partial_y + c^*(\varepsilon)] f_\pm^R(-\varepsilon) &= \mp s^*(\varepsilon) e^{i\theta_u}, \\ [\zeta\partial_y + c^*(\varepsilon)][f_\pm^R(\varepsilon)]^* &= \pm s^*(\varepsilon) e^{-i\theta_u}. \end{aligned} \tag{12}$$

In the equilibrium conditions, the current density vector is given by the Keldysh block as

$$\mathbf{J}(\mathbf{R}) = J_0 \int d\varepsilon \mathrm{Tr}\{\rho_3(\hat{G}[\hat{\partial}, \hat{G}])^K\}, \tag{13}$$

where J_0 is a normalization constant. The current density vector determines the direction and amplitude of the current density inside the sandwiched layer as a function of coordinates. If we substitute the total Green's function Eq. (1) into the current density relation, namely, Eq. (13), we arrive at

$$\begin{aligned} \mathbf{J}(\mathbf{R}) = J_0 \int_{-\infty}^{\infty} d\varepsilon \tanh(\varepsilon\beta)\{ & f_-^R(-\varepsilon)\vec{\nabla}[f_+^R(\varepsilon)]^* \\ & + f_+^R(-\varepsilon)\vec{\nabla}[f_-^R(\varepsilon)]^* - f_+^R(\varepsilon)\vec{\nabla}[f_-^R(-\varepsilon)]^* \\ & - f_-^R(\varepsilon)\vec{\nabla}[f_+^R(-\varepsilon)]^* + [f_-^R(-\varepsilon)]^*\vec{\nabla} f_+^R(\varepsilon) \\ & + [f_+^R(-\varepsilon)]^*\vec{\nabla} f_-^R(\varepsilon) - [f_+^R(\varepsilon)]^*\vec{\nabla} f_-^R(-\varepsilon) \\ & - [f_-^R(\varepsilon)]^*\vec{\nabla} f_+^R(-\varepsilon)\}. \end{aligned} \tag{14}$$

To obtain the total supercurrent flowing through the junction, for example, at the right superconducting gate, one needs to perform an integration of Eq. (13) over the y coordinate, $I(\phi) = I_0 \int\int dy d\varepsilon \mathrm{Tr}\{\rho_3(\check{g}[\hat{\partial}, \check{g}])^K\}$.

At this point it suffices that Eqs. (5) be solved together with appropriate boundary conditions [i.e., Eqs. (9)–(12)] in order to capture the transport characteristics of the present class of Josephson junctions in the diffusive limit.

B. Analytical microscopic discussions

In this section we derive explicit analytical expressions describing the supercurrent at each superconducting terminal. To this end, we consider the weak proximity limit of the diffusive regime where the Keldysh-Usadel method yields a set of uncoupled complex elliptic partial differential equations. The simplified Usadel equations and corresponding boundary conditions are given by Eqs. (5), (6), (9), (10), (11), and (12). For simplicity in our analytical calculations we exclude first-order terms of the anomalous Green's function in the Kupryianov-Lukichev boundary conditions, Eq. (7). We use the Fourier series method in the presence of nonhomogeneous

boundary conditions and obtain analytical solutions for the Usadel equations. The method leads to somewhat lengthy solutions; for instance, one of the anomalous components of the Green's function, namely, $f_+^R(\varepsilon)$, after long calculations is given by Eq. (15):

$$f_+^R(\varepsilon) = -\left\{\frac{\Delta \mathrm{sgn}(\varepsilon)}{\sqrt{\varepsilon^2-\Delta^2}}\Theta(\varepsilon^2-\Delta^2) - \frac{i\Delta}{\sqrt{\Delta^2-\varepsilon^2}}\Theta(\Delta^2-\varepsilon^2)\right\}\left\{\frac{e^{i\theta_l}}{L\zeta}\left(x - \frac{x^2}{2L} + \frac{D}{2iL(\varepsilon+h)} - \frac{L}{3}\right.\right.$$
$$\left. - \sum_{k=1}^{\infty}\frac{4iL(\varepsilon+h)\cos(\frac{k\pi x}{L})}{k^2\pi^2[Dk^2\pi^2/L^2 - 2i(\varepsilon+h)]}\right) - \frac{e^{i\theta_r}}{L\zeta}\left(\frac{x^2}{2L} - \frac{D}{2iL(\varepsilon+h)} - \frac{L}{6} + \sum_{k=1}^{\infty}\frac{4iL(\varepsilon+h)(-1)^k\cos(\frac{k\pi x}{L})}{k^2\pi^2[Dk^2\pi^2/L^2 - 2i(\varepsilon+h)]}\right)$$
$$+\frac{e^{i\theta_d}}{W\zeta}\left(y - \frac{y^2}{2W} + \frac{D}{2iW(\varepsilon+h)} - \frac{W}{3} - \sum_{l=1}^{\infty}\frac{4iW(\varepsilon+h)\cos(\frac{l\pi y}{W})}{l^2\pi^2[Dl^2\pi^2/W^2 - 2i(\varepsilon+h)]}\right) - \frac{e^{i\theta_u}}{W\zeta}\left(\frac{y^2}{2W} - \frac{D}{2iW(\varepsilon+h)}\right.$$
$$\left.\left. - \frac{W}{6} + \sum_{l=1}^{\infty}\frac{4iW(\varepsilon+h)(-1)^l\cos(\frac{l\pi y}{W})}{l^2\pi^2[Dl^2\pi^2/W^2 - 2i(\varepsilon+h)]}\right)\right\}. \tag{15}$$

The length and width of the ferromagnetic region sandwiched between the superconductors are denoted by L and W, respectively. As can be seen, the anomalous component of the retarded Green's function depends on all four condensation phases, which in turn leads to an interference between these superconducting phases in the Josephson current. In Eq. (14) there are eight different terms of anomalous components of the Green's function involved in the supercurrent relation. Therefore, one must find eight solutions similar to Eq. (15) for other terms and substitute them into the supercurrent relation Eq. (14) in order to obtain the supercurrent at one terminal. To obtain analytical solutions for the total supercurrent flowing at the other superconducting terminals, one must repeat the latter described process. We have done so and arrived at the analytical expressions describing the supercurrent in the system as follows. The supercurrent at $x = 0, L$ terminals is obtained as

$$\frac{I_x(x=0)}{I_0} = \int_{-\infty}^{\infty}\frac{d\varepsilon}{\Delta_0}\frac{\Delta^2\tanh(\beta\varepsilon)}{\Delta^2-\varepsilon^2}\sum_{\sigma=\pm}\left\{\left(\frac{WD}{L^3\zeta^2(\varepsilon+\sigma h)} + \frac{8WD}{L^3\zeta}\sum_{k=1}^{\infty}\frac{(-1)^k(\varepsilon+\sigma h)}{D^2k^4\pi^4/L^4 + 4(\varepsilon+\sigma h)^2}\right)\sin(\theta_l-\theta_r)\right.$$
$$\left. + \frac{D\sin(\theta_l-\theta_u)}{LW\zeta^2(\varepsilon+\sigma h)} + \frac{D\sin(\theta_l-\theta_d)}{LW\zeta^2(\varepsilon+\sigma h)}\right\}, \tag{16}$$

$$\frac{I_x(x=L)}{I_0} = \int_{-\infty}^{\infty}\frac{d\varepsilon}{\Delta_0}\frac{\Delta^2\tanh(\beta\varepsilon)}{\Delta^2-\varepsilon^2}\sum_{\sigma=\pm}\left\{\left(\frac{WD}{L^3\zeta^2(\varepsilon+\sigma h)} + \frac{8WD}{L^3\zeta}\sum_{k=1}^{\infty}\frac{(-1)^k(\varepsilon+\sigma h)}{D^2k^4\pi^4/L^4 + 4(\varepsilon+\sigma h)^2}\right)\sin(\theta_l-\theta_r)\right.$$
$$\left. + \frac{D\sin(\theta_d-\theta_r)}{LW\zeta^2(\varepsilon+\sigma h)} + \frac{D\sin(\theta_u-\theta_r)}{LW\zeta^2(\varepsilon+\sigma h)}\right\}. \tag{17}$$

And also at the $W = 0, L$ terminals,

$$\frac{I_y(y=0)}{I_0} = \int_{-\infty}^{\infty}\frac{d\varepsilon}{\Delta_0}\frac{\Delta^2\tanh(\beta\varepsilon)}{\Delta^2-\varepsilon^2}\sum_{\sigma=\pm}\left\{\left(\frac{LD}{W^3\zeta^2(\varepsilon+\sigma h)} + \frac{8LD}{W^3\zeta}\sum_{l=1}^{\infty}\frac{(-1)^l(\varepsilon+\sigma h)}{D^2l^4\pi^4/W^4 + 4(\varepsilon+\sigma h)^2}\right)\sin(\theta_d-\theta_u)\right.$$
$$\left. + \frac{D\sin(\theta_d-\theta_r)}{LW\zeta^2(\varepsilon+\sigma h)} + \frac{D\sin(\theta_d-\theta_l)}{LW\zeta^2(\varepsilon+\sigma h)}\right\}, \tag{18}$$

$$\frac{I_y(y=W)}{I_0} = \int_{-\infty}^{\infty}\frac{d\varepsilon}{\Delta_0}\frac{\Delta^2\tanh(\beta\varepsilon)}{\Delta^2-\varepsilon^2}\sum_{\sigma=\pm}\left\{\left(\frac{LD}{W^3\zeta^2(\varepsilon+\sigma h)} + \frac{8LD}{W^3\zeta}\sum_{l=1}^{\infty}\frac{(-1)^l(\varepsilon+\sigma h)}{D^2l^4\pi^4/W^4 + 4(\varepsilon+\sigma h)^2}\right)\sin(\theta_d-\theta_u)\right.$$
$$\left. + \frac{D\sin(\theta_l-\theta_u)}{LW\zeta^2(\varepsilon+\sigma h)} + \frac{D\sin(\theta_r-\theta_u)}{LW\zeta^2(\varepsilon+\sigma h)}\right\}. \tag{19}$$

In the preceding equations, $\sigma = \pm$ comes from the spin-dependent nature of the ferromagnetic material which is sandwiched between the four superconducting terminals. To be more specific, $I_x(x=0)$, $I_x(x=L)$, $I_y(y=0)$, and $I_y(y=W)$ represent the Josephson current in the x direction at $x = 0, L$ and in the y direction at $y = 0, W$, respectively. The above currents involve three sinusoidal terms whose arguments include phase differences of the lead the supercurrent is being calculated at and the three other terminals. As expected, the obtained supercurrents show explicitly that these interfering terms in the x and y directions vanish for large L and W, respectively. This fact is also found in ballistic junctions.[26,32] In these two limits, either large L or large W, the system takes on quasi-one-dimensional features and we recover the well-known standard sinusoidal Josephson relation for the supercurrent. However, in the opposite regime where $L \simeq W$, the proximity-induced order parameters from the superconducting terminals overlap substantially and additional terms compared to the one-dimensional case appear in the expressions for the supercurrent. As we show, the supercurrent can behave very differently from one-dimensional junctions as a function of the phase in one superconducting terminal

due to this overlap. In fact, the supercurrent is a function of a superposition of sinusoidal phase differences between the different superconducting leads, and one may express the supercurrent relations as $I(x_i) = \sum_j I_j \sin(\theta_i - \theta_j)$ in weakly coupled systems.[26,29–32] The conservation of the charge current is also satisfied by the current relationships, namely, Eqs. (16)–(19). It can be verified explicitly that

$$I_x(x = 0) + I_y(y = 0) = I_x(x = L) + I_y(y = W), \quad (20)$$

which constitutes the Kirchhoff law of electricity. We proceed to investigate and justify the obtained analytical supercurrent *numerically* and study how it depends on the superconducting phases of the terminals. First, we compare our analytical expressions for the supercurrent with the results obtained via a macroscopic Ginzburg-Landau theory in the next section.

C. Ginzburg-Landau approach: Analytical macroscopic discussions

In this section, we make a complementary discussion and examine qualitatively the quasiclassical findings of the previous section by comparison with a phenomenological Ginzburg-Landau (GL) theory.[38] The phenomenological approach is a macroscopic theory which is unable to explain the microscopic mechanism underlying superconductivity but instead describes the macroscopic properties near a phase transition of the system by writing the free energy as an expansion in the order parameter. We note that the smallness of the superconducting order parameter may be compared directly with the weak proximity effect regime in the quasiclassical theory for temperatures near T_c. We assume here that the normal region's characteristic length scale (d) satisfies $\xi \gg d$, where ξ is the coherence length. In this case the condensation wave functions overlap effectively via the proximity effect. It is instructive to briefly consider first the one-dimensional case, where one may write an ansatz for the wave function as follows[4,39]:

$$\psi = \psi_1 e^{i\theta_1}\mathcal{X} + \psi_2 e^{i\theta_2}(1 - \mathcal{X}). \quad (21)$$

Here, ψ_j is the amplitude of the condensate wave function in the region $j = 1,2$ while θ_j is the corresponding superconducting phase. The function $\mathcal{X}$ is unknown, but it is assumed to satisfy $\mathcal{X} \to 1$ inside region 1 and $\mathcal{X} \to 0$ inside region 2. We now generalize this ansatz to the present four-terminal two-dimensional case. Assume that deep inside the superconducting banks the order parameter is given as

$$\psi = \psi_u e^{i\theta_u},\ \psi_d e^{i\theta_d},\ \psi_l e^{i\theta_l},\ \psi_r e^{i\theta_r}. \quad (22)$$

Inside the contact region, the four condensations' wave functions overlap and consequently we expect a solution as

$$\begin{aligned}\psi = {} & \psi_r e^{i\theta_r}\mathcal{X}\mathcal{Y}(1 - \mathcal{Y}) + \psi_l e^{i\theta_l}(1 - \mathcal{X})\mathcal{Y}(1 - \mathcal{Y}) \\ & + \psi_u e^{i\theta_u}\mathcal{Y}\mathcal{X}(1 - \mathcal{X}) + \psi_d e^{i\theta_d}(1 - \mathcal{Y})\mathcal{X}(1 - \mathcal{X}),\end{aligned} \quad (23)$$

where we have generalized the mentioned one-dimensional ansatz for the four-terminal junction. The functions $\mathcal{X}$ and $\mathcal{Y}$ satisfy the following asymptotic behavior: $\mathcal{X} \to 0$ in the left, $\mathcal{X} \to 1$ in the right, $\mathcal{Y} \to 0$ in the bottom, and $\mathcal{Y} \to 1$ in the top superconductors. The supercurrent density can now be defined by the second GL equation,[4,39]

$$\mathbf{j}_s = \frac{\alpha\hbar e}{\beta m}\mathrm{Im}\{\psi^*\nabla\psi\}, \quad (24)$$

where α and β are phenomenological coefficients in the GL theory. After some calculations, we find the following expressions for j_x and j_y, the supercurrent components in the x and y directions:

$$\begin{aligned}\mathrm{j}_x = {} & \mathcal{X}'(1 - \mathcal{Y})\mathcal{Y}\{-\mathcal{Y}(1 - \mathcal{Y})\psi_l\psi_r \sin(\theta_l - \theta_r) \\ & - \mathcal{X}^2(1 - \mathcal{Y})\psi_d\psi_r \sin(\theta_d - \theta_r) - \mathcal{X}^2\mathcal{Y}\psi_u\psi_r \\ & \times \sin(\theta_u - \theta_r) + (1 - \mathcal{X})^2(1 - \mathcal{Y})\psi_d\psi_l \sin(\theta_d - \theta_l) \\ & + \mathcal{Y}(1 - \mathcal{X})^2\psi_u\psi_l \sin(\theta_u - \theta_l)\},\end{aligned} \quad (25)$$

$$\begin{aligned}\mathrm{j}_y = {} & \mathcal{Y}'(1 - \mathcal{X})\mathcal{X}\{-\mathcal{X}(1 - \mathcal{X})\psi_u\psi_d \sin(\theta_u - \theta_d) \\ & - \mathcal{Y}^2(1 - \mathcal{X})\psi_l\psi_u \sin(\theta_l - \theta_u) - \mathcal{Y}^2\mathcal{X}\psi_r\psi_u \\ & \times \sin(\theta_r - \theta_u) + (1 - \mathcal{Y})^2(1 - \mathcal{X})\psi_l\psi_d \sin(\theta_l - \theta_d) \\ & + \mathcal{X}(1 - \mathcal{Y})^2\psi_d\psi_r \sin(\theta_r - \theta_d)\},\end{aligned} \quad (26)$$

in which the prime denotes derivation. The obtained results illustrate that, for instance in j_x, the terms coupling the top and bottom superconducting terminals vanish. In this way, we see that the phenomenological GL approach produces identical dependencies on the superconducting phase differences as the microscopic approach using quasiclassical theory. Direct comparison with, e.g., Eqs. (16) and (17) in the appropriate limits for $\mathcal{X}$ shows consistency with Eq. (25).

III. FOUR-TERMINAL NONMAGNETIC JOSEPHSON JUNCTION

In this section, we first set $h = 0$ (the exchange field of the ferromagnetic layer) and consider an S/N/S junction. Basically, there are two methods for inducing a supercurrent into our Josephson system: (1) via an external flux where the external magnetic field penetrates the junction through a superconducting quantum interference device (SQUID)-like geometry and (2) via a current bias where the supercurrent is injected into the system. A combination of these two methods is also possible by utilizing different configurations of a multiterminal system (for a comprehensive investigation of such possibilities, see Refs. 26,29–32,43). The supercurrent at each terminal can be generally expressed as $I_i = \sum_{i,j} I_{i,j} \sin(\theta_i - \theta_j)$. Thus if one is able to tune the superconducting phases independently, the supercurrent will be a 2π-periodic function of one of the superconducting phases.

Numerical justification of current-phase relationships

In this section, we discuss the analytical findings obtained in the previous section and present numerical results using a real energy representation. In the actual plots, we consider a temperature $T = 0.05T_c$ and also set the normal region's length and width to $L = W \simeq 2.5\xi_S$. In this representation, we normalize lengths against ξ_S and introduce the Thouless energy $\varepsilon_T = (\hbar D/L^2)$. Also, we have normalized the quasiparticles' energy by the superconducting gap at zero temperature, Δ_0,

and consider units so that $\hbar = k_B = 1$. Moreover, we add a small imaginary number $\eta/\Delta_0 = 0.1$ to the quasiparticle energy to account for inelastic scattering, which leads to a finite lifetime for quasiparticle excitations. Setting $\zeta = 7$ ensures the validity of weak proximity in numerical calculations. Solving numerically the resultant complex boundary-value partial differential equations, the approximate solution components of the Usadel equation are assumed to be linear combinations of bicubic Hermite basis functions. They are required to satisfy the Usadel equations (5) and (6) exactly at four collocation points in each subrectangle of a grid, and to satisfy the boundary conditions exactly at certain boundary collocation points. We mention in passing that we include first-order terms of the anomalous Green's function in the Kupryianov-Lukichev boundary conditions, as was done in Ref. 40, in contrast to the usual approximation in the literature where such terms are discarded. By doing so, we improve the accuracy of the analytical solution in our numerical investigations. Finally, the linear algebraic equations resulting from the collocation method, which are highly nonsymmetric and thus difficult to solve using iterative and sparse direct solvers, are solved using a Jacobi conjugate-gradient method, which means that the conjugate gradient method (Sec. 4.8 of Ref. 41) is applied to the preconditioned normal equations $D^{-1}A^TA\mathbf{x} = D^{-1}A^T\mathbf{b}$, where D is the diagonal part of A^TA. For a generalized discussion see Ref. 42. The same framework was very recently used in Ref. 34 to study the anomalous Fraunhofer pattern appearing in an inhomogeneous S/F/S structure.

In order to clarify the behavior of the supercurrent in the present four-terminal Josephson junction with respect to condensate phases of the four superconductors, we use the following strategy. We focus on the behavior of the supercurrent with respect to one superconductor's phase (the left one) and set two phases equal to zero ($\theta_{\text{down}} = \theta_{\text{right}} = 0$), while varying θ_{up}. The motivation for this is to see if the supercurrent flowing in one direction can be tuned explicitly by the superconducting phase difference in the transverse direction, which would correspond to a superconducting-phase-transistor-like device.

In general, the supercurrent inside the normal diffusive region is described by a vector field and depends on the position. The total flowing current is conserved, as we have proven analytically. We focus here on the supercurrent flowing into and out of the terminals, i.e., at the positions $x = 0$, $y = 0$, $x = L$, and $y = W$ gates. The results are shown in Fig. 2, where we plot the supercurrent at the four gates as a function of the left superconducting phase where θ_u is varied while $\theta_d = \theta_r = 0$. The top left frame shows the supercurrent at $x = 0$ as a function of the left superconducting phase, the top right is the supercurrent at $x = L$, the bottom left frame displays the supercurrent at $y = 0$, and finally the bottom right frame shows the supercurrent at $y = W$. The standard sinusoidal current-phase relation appears at all gates in the special case where θ_u is equal to zero. This behavior can be understood by considering Eqs. (16)–(19). In this case, only terms with $\sin(\theta_l)$ survive and the supercurrent exhibits a pure sinusoidal relation versus θ_l. When θ_u increases, the phase shift effectively adds a constant which can be either positive or negative. In particular, the currents at $x = L$ and $y = 0$ shift either upward or downward depending on the value of θ_u, as

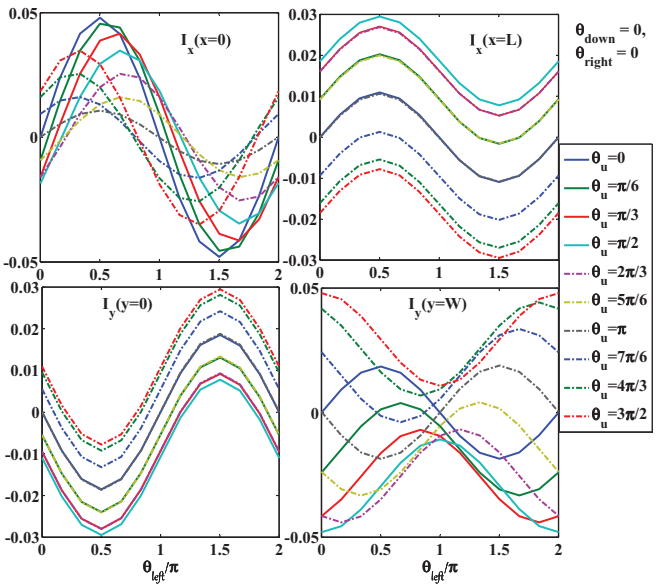

FIG. 2. (Color online) Top left: Supercurrent in the x direction as a function of left condensation phase, θ_{left}, at left superconductor gate, i.e., $x = 0$. Top right: Supercurrent in the x direction vs left superconducting phase, θ_{left}, at right superconductor gate, i.e., $x = L$. Bottom left: Supercurrent in the y direction as a function of left condensation phase at down superconductor gate, i.e., $y = 0$. Bottom right: Supercurrent in the y direction vs left superconducting phase at up gate, i.e., $y = W$. Here other superconductor phases, namely θ_{up} and θ_{down}, are assumed to be zero.

can be understood by looking at Eqs. (17) and (18): a change in θ_u only varies constant terms involving $\sin(\theta_u)$.

In contrast, variation in θ_u influences the currents at $x = 0$ and $y = W$ in a more complicated manner. In this case, there is an explicit dependence on the phase difference $\theta_l - \theta_u$, which induces a strongly nonsinusoidal behavior in the current-phase relation. Interestingly, we see that it is possible to cancel out the current even for a finite value of θ_l by choosing θ_u appropriately. This observation suggests that the present four-terminal device can act as a superconducting phase transistor, where the phase difference in one direction controls the supercurrent flowing in the perpendicular direction. The underlying mechanism behind this is the interference between the condensate wave functions in the diffusive normal region, which results in an intricate phase dependence of the supercurrent as shown in the analytical results.

IV. FOUR-TERMINAL MAGNETIC JOSEPHSON JUNCTION

In this section, we consider a four-terminal Josephson junction with a ferromagnetic barrier where the exchange field of the magnetic layer is oriented along the z direction. In the usual two-terminal magnetic Josephson junctions, an increment of the ferromagnetic barrier thickness not only reverses the current direction at particular thicknesses but also renders the minimum of junction energy to change from 0 superconducting phase difference to a π phase. The phenomenon is the so-called 0-π transition. As discussed in Ref. 26, the junction energy where there are several superconducting leads

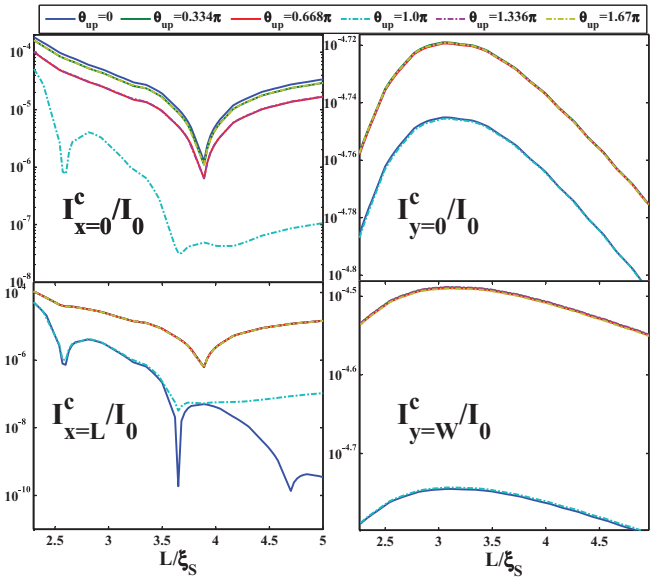

FIG. 3. (Color online) Critical supercurrent as a function of the normalized junction length L/ξ_S at different superconducting gates and for various values of $\theta_{\rm up}$, the superconducting phase of the up terminal. Top left: At the left superconductor gate, i.e., $x = 0$. Top right: At the right superconductor gate, i.e., $x = L$. Bottom left: At the down superconductor gate, i.e., $y = 0$. Bottom right: At the up gate, i.e., $y = W$. The other superconductor phases are fixed at zero.

can be expressed as $E_J = \sum_{j<i} \gamma_{j,i}[1 - \cos(\theta_j - \theta_i)]$. Here, the i and j indices stand for the ith and jth superconducting leads. Below we demonstrate that an increment in the thickness of the ferromagnet can reverse the flow of the supercurrent into a pair of the superconducting terminals (along the direction of increment), whereas the current direction in the other terminal pair remains unaltered.

The behavior of critical supercurrent as a function of magnetic barrier thickness

We here present a *numerical* study of the transport properties of four-terminal ferromagnetic Josephson junctions. Although the numerical results are confirmed by the analytical expressions presented in Sec. III, we include first-order terms of the anomalous Green's function in the Kupryianov-Lukichev boundary conditions in contrast to the approximation used for deriving the analytical expressions for supercurrent where such terms are dropped. We now consider a nonzero value of the ferromagnetic exchange field h. For a weak, diffusive ferromagnetic alloy such as Pd_xNi_{1-x}, the exchange field h/Δ_0 is tunable by means of the doping level x to take values in the range meV to tens of meV. Here we fix $h = 10\Delta_0$, which typically places the exchange field h in the range 10–20 meV. In order to investigate the effects of magnetic barrier thickness on the supercurrent at each terminal and the influence of the various superconducting phases, we follow a similar strategy as in the previous section: θ_l is varied from 0 to 2π, where magnetic barrier length, L, is being varied from $L = 2\xi_S$ to $L = 5\xi_S$. The other superconducting phases are fixed at zero except θ_u, which is changed in order to demonstrate the possible influence of the other superconducting phases. The critical value of the supercurrent at each terminal is calculated separately for each value of θ_u.

Figure 3 indicates the behavior of the critical supercurrent at each superconductor lead as a function of normalized junction length L/ξ_S for various values of θ_u. The top left frame exhibits the critical current at the left terminal. Except for $\theta_u = \pi$, which shows two points changing the supercurrent direction, the other values give rise to one sign change in the critical current. Identical qualitative behavior appears for the current at the right terminal except when $\theta_u = 0$, as shown in the bottom left frame. The top and bottom right frames exhibit the critical supercurrent versus L/ξ_S at the down and up terminals, respectively. The critical supercurrent at the two terminals shows a smooth function of L/ξ_S, which is in stark contrast with the behavior of the critical supercurrent at the left and right terminal. Thus, the increment of the junction length primarily affects the critical supercurrent flowing into leads along the same direction of the increment. Moreover, the direction of the current can be switched by tuning the superconducting phase of up terminal. In contrast, the current flowing into the superconducting banks perpendicular to the junction length increment is left unchanged. This class of multiterminal ferromagnet Josephson junction then offers an interesting synthesis between 0 and π states, and possibly ϕ states, due to the fact that the coefficients I_j can change sign depending on the junction parameters such as L and W.

V. CONCLUSIONS

In conclusion, we have studied a four-terminal Josephson junction where a diffusive normal or ferromagnetic metal with sides L and W is sandwiched among four s-wave superconductor leads. We have obtained explicit analytical results using the quasiclassical Keldysh-Usadel method for the supercurrent in the system. We find that the wave functions of the four superconductors interfere efficiently when $L \simeq W$ and modify the standard sinusoidal current-phase relation, which confirms previous findings in ballistic junctions. These findings are confirmed qualitatively by using a macroscopic Ginzburg-Landau theory. We have presented numerical results for the behavior of the supercurrent, and demonstrated that the current flowing along one axis may be tuned by the superconducting phase difference along the perpendicular direction. It is demonstrated that such four-terminal junctions can provide a rich switching circuit element (due to additional degrees of freedom in comparison with one-dimensional two-terminal Josephson junctions) where the various superconducting phases influence considerably the current behavior at the terminals. In particular, we show that a reversal in critical current direction as a function of junction length can be switched by means of variation of the superconducting phase of perpendicular terminals. The present investigations of diffusive cruciate magnetic Josephson junctions may provide new perspectives for the design of superconducting phase switches that can be used in quantum circuits as switching elements.

ACKNOWLEDGMENTS

The authors would like to thank K. Halterman for his generosity regarding compiler source and also F. S. Bergeret for fruitful discussions.

*phymalidoust@gmail.com
†sewell@utep.edu
‡jacob.linder@ntnu.no

[1]B. D. Josephson, Phys. Lett. **1**, 251 (1962).
[2]I. K. Yason, V. M. Svistunov, and I. M. Dmitrenko, Zh. Eksp. Teor. Fiz. **48**, 976 (1965) [Sov. Phys. JETP **21**, 650 (1965)].
[3]S. Shapiro, Phys. Rev. Lett. **11**, 80 (1965).
[4]K. K. Likharev, Rev. Mod. Phys. **51**, 101 (1979).
[5]A. A. Golubov, M. Yu. Kupriyanov, and E. Ilichev, Rev. Mod. Phys. **76**, 411 (2004).
[6]A. I. Buzdin, Rev. Mod. Phys. **77**, 935 (2005).
[7]F. S. Bergeret, A. F. Volkov, and K. B. Efetov, Rev. Mod. Phys. **77**, 1321 (2005).
[8]W. L. McMillan, Phys. Rev. **175**, 537 (1968).
[9]W. Belzig, C. Bruder, and G. Schön, Phys. Rev. B **54**, 9443 (1996).
[10]J. C. Hammer, J. C. Cuevas, F. S. Bergeret, and W. Belzig, Phys. Rev. B **76**, 064514 (2007).
[11]J. C. Cuevas, J. Hammer, J. Kopu, J. K. Viljas, and M. Eschrig, Phys. Rev. B **73**, 184505 (2006).
[12]H. le Sueur, P. Joyez, H. Pothier, C. Urbina, and D. Esteve, Phys. Rev. Lett. **100**, 197002 (2008).
[13]M. Alidoust, G. Rashedi, J. Linder, and A. Sudbø, Phys. Rev. B **82**, 014532 (2010).
[14]F. Giazotto, J. T. Peltonen, M. Meschke, and J. P. Pekola, Nat. Phys. **6**, 254 (2010).
[15]M. S. Crosser, J. Huang, F. Pierre, P. Virtanen, T. T. Heikkilä, F. K. Wilhelm, and N. O. Birge, Phys. Rev. B **77**, 014528 (2008).
[16]J. J. A. Baselmans, A. F. Morpurgo, B. J. van Wees, and T. M. Klapwijk, Nature (London) **397**, 43 (1999).
[17]Jian Huang, F. Pierre, Tero T. Heikkila, Frank K. Wilhelm, and Norman O. Birge, Phys. Rev. B **66**, 020507(R) (2002).
[18]A. I. Buzdin, L. N. Bulaevskii, and S. V. Panyukov, Pisma Zh. Eksp. Teor. Fiz. **35**, 147 (1982) [JETP Lett. **35**, 178 (1982)]; A. I. Buzdin and M. Y. Kuprianov, Pisma Zh. Eksp. Teor. Fiz. **53**, 308 (1991) [JETP Lett. **53**, 321 (1991)].
[19]J. S. Jiang, D. Davidovic, D. H. Reich, and C. L. Chien, Phys. Rev. Lett. **74**, 314 (1995).
[20]A. S. Sidorenko, V. I. Zdravkov, A. A. Prepelitsa, C. Helbig, Y. Luo, S. Gsell, M. Schreck, S. Klimm, S. Horn, L. R. Tagirov, and R. Tidecks, Ann. Phys. **12**, 37 (2003).
[21]I. A. Garifullin, D. A. Tikhonov, N. N. Garifyanov, L. Lazar, Yu. V. Goryunov, S. Ya. Khlebnikov, L. R. Tagirov, K. Westerholt, and H. Zabel, Phys. Rev. B **66**, 020505(R) (2002).
[22]V. A. Oboznov, V. V. Bolginov, A. K. Feofanov, V. V. Ryazanov, and A. I. Buzdin, Phys. Rev. Lett. **96**, 197003 (2006).
[23]M. Faure, A. I. Buzdin, A. A. Golubov, and M. Yu. Kupriyanov, Phys. Rev. B **73**, 064505 (2006).
[24]J. Linder, T. Yokoyama, and A. Sudbø, Phys. Rev. B **77**, 174514 (2008).
[25]M. Alidoust, J. Linder, G. Rashedi, T. Yokoyama, and A. Sudbø, Phys. Rev. B **81**, 014512 (2010).
[26]M. Zareyan and A. N. Omelyanchouk, J. Low Temp. Phys. **25**, 175 (1999).
[27]M. H. S. Amin, A. N. Omelyanchouk, and M. Zagoskin, Physica C **372**, 178 (2002); M. H. S. Amin, A. N. Omelyanchouk, A. Blais, Alec Maassen van den Brink, G. Rose, T. Duty, and A. M. Zagoskin, *ibid.* **368**, 310 (2002).
[28]F. S. Bergeret and J. C. Cuevas, J. Low. Temp. Phys. **153**, 304 (2008).
[29]R. de Bruyn Ouboter, A. N. Omelyanchouk, and E. D. Vol, Physica B **205**, 153 (1995).
[30]B. j. Vleeming, A. V. Zakarian, A. N. Omelyanchouk and R. de Bruyn Ouboter, Physica B **226**, 253 (1996); B. j. Vleeming, F. J. C. van Bemmelen, M. R. Berends, R. de Bruyn Ouboter, and A. N. Omelyanchouk, *ibid.* **262**, 296 (1999).
[31]R. de Bruyn Ouboter, and A. N. Omelyanchouk, Superlattice Mircrostruct. **25**, 1005 (1999).
[32]A. N. Omelyanchouk and M. Zareyan, Physica B + C **81**, 291 (2000).
[33]M. H. S. Amin, A. N. Omelyanchouk, and M. Zagoskin, J. Low Temp. Phys. **27**, 616 (2001).
[34]M. Alidoust, G. Sewell, and J. Linder, Phys. Rev. Lett. **108**, 037001 (2012).
[35]K. D. Usadel, Phys. Rev. Lett. **25**, 507 (1970); A. I. Larkin and Y. N. Ovchinnikov, in *Nonequilibrium Superconductivity*, edited by D. Langenberg and A. Larkin (Elsevier, Amesterdam, 1986), p. 493.
[36]J. P. Morten, M.Sc. thesis, Norwegian University of Science and Technology, 2003.
[37]A. V. Zaitsev, Zh. Eksp. Teor. Fiz. **86**, 1742 (1984) [Sov. Phys. JETP **59**, 1015 (1984)]; M. Y. Kuprianov *et al.*, *ibid.* **67**, 1163 (1988).
[38]V. L. Ginzburg and L. D. Landau, Zh. Eksp. Teor. Fiz. **20**, 1064 (1950).
[39]L. G. Aslamazov and A. I. Larkin, Pis'ma Zh. Eksp. Teor. Fiz. **48**, 976 (1965).
[40]I. B. Sperstad, J. Linder, and A. Sudbø, Phys. Rev. B **78**, 104509 (2008).
[41]G. Sewell, *The Numerical Solution of Ordinary and Partial Differential Equations*, 2nd ed. (Wiley, New York, 2005).
[42]G. Sewell, Adv. Eng. Software **41**, 748 (2010).
[43]R. de Bruyn Ouboter and A. N. Omelyanchouk, Physica C **254**, 134 (1998).